CHAPTER FIVE

Designed Ankyrin Repeat Proteins (DARPins): From Research to Therapy

Rastislav Tamaskovic, Manuel Simon, Nikolas Stefan, Martin Schwill, *and* Andreas Plückthun

Contents

Department of Biochemistry, University of Zurich, Winterthurerstrasse, Zurich, Switzerland

Methods in Enzymology, Volume 503
ISSN 0076-6879, DOI: 10.1016/B978-0-12-396962-0.00005-7

Abstract

Designed ankyrin repeat proteins (DARPins) have been developed into a robust and versatile scaffold for binding proteins. High-affinity binders are routinely selected by ribosome display and phage display. DARPins have entered clinical trials and have found numerous uses in research, due to their high stability and robust folding, allowing many new molecular formats. We summarize the DARPin properties and highlight some biomedical applications. Protocols are given for labeling with dyes and polyethylene glycol, for quantitatively measuring binding to cell surface receptors by kinetics and thermodynamics, and for exploiting new engineering opportunities from using "click chemistry" with nonnatural amino acids.

1. Introduction

1.1. Background

To embark on developing a new protein scaffold class as a general binding module, there has to be a strong motivation, especially when carried out in a laboratory with a long-standing focus on antibody engineering and technology (Glockshuber *et al.*, 1990; Skerra and Plückthun, 1988). As the designed ankyrin repeat protein (DARPin) technology was developed in an academic setting (Binz *et al.*, 2003; Forrer *et al.*, 2003), the driving force was the desire to create a scaffold with superior technological properties.

Through the design of a fully synthetic antibody library (Knappik *et al.*, 2000) and the development of ribosome display (Hanes and Plückthun, 1997; Hanes *et al.*, 1998), which incorporates affinity maturation and directed evolution directly in the workflow, the basic operation of both natural antibody generation and somatic mutation had been replicated in the laboratory. Ironically, the antibody molecule was then no longer needed, and the technology had become independent of its roots. From extensive experiments with the engineering of antibodies and their fragments (Wörn and Plückthun, 2001), it had become evident that the molecules themselves contain some technical limitations.

Today, recombinant antibody scFv or Fab fragments are usually converted back to an IgG for therapeutic applications (Plückthun and Moroney, 2005), and the biophysical properties (or "developability") of a particular antibody are an important consideration. When using the antibody fragments in more ambitious formats (as fusions to other aggregation-prone proteins, in multimers, or in the absence of disulfide bonds), the limitations in their biophysical properties become even more apparent.

1.2. Properties of repeat proteins

Repeat proteins appeared very attractive as a choice for a general binding protein. Repeat proteins (Kobe and Kajava, 2000) contain modules, whose number can be chosen freely, which stack up on each other to create a rigid protein domain. They have different architectures, but within one family, they use modules of almost identical structure but with individual surfaces to specifically bind their target. After engineering work on the repeat proteins had started (Binz *et al.*, 2003; Forrer *et al.*, 2003; Stumpp *et al.*, 2003), the discovery that jawless vertebrates use an adaptive immune system made of leucine-rich repeat proteins (Pancer *et al.*, 2004) came as a surprising validation of the concept.

Repeat proteins seem to follow rules which can be derived from biophysical considerations: a large interaction surface is usually a prerequisite for tight binding. Such a binding interface should be rigid, in order to not lose entropy upon binding, which would otherwise decrease the overall achievable binding free energy (equivalent to a loss in affinity). Also, the surface should be modular and thus "patches" should be individually exchangeable or modifiable by affinity maturation. Furthermore, the protein should also not require disulfides, to have the option of expressing it in the bacterial cytoplasm, and to later introduce unique cysteines for site-specific coupling with drugs, fluorescent labels, or polyethylene glycol (PEG), just to name a few.

1.3. Properties of DARPins

Ankyrin repeat proteins (Bork, 1993; Li *et al.*, 2006) are built from tightly joined repeats of usually 33 amino acid residues. Each repeat forms a structural unit consisting of a β-turn followed by two antiparallel α-helices (Fig. 5.1), and up to 29 consecutive repeats can be found in a single protein (Walker *et al.*, 2000). Yet, ankyrin repeat domains usually consist of four to six repeats, which stack onto each other, leading to a right-handed solenoid structure with a continuous hydrophobic core and a large solvent accessible surface (Kobe and Kajava, 2000; Sedgwick and Smerdon, 1999).

We exploited the huge available sequence information of the repeats within the protein family (different protein variants each with several repeats) by using a "consensus" strategy (Forrer *et al.*, 2004). The underlying assumption is that residues important for maintaining the fold will be more conserved and thus show up prominently in an alignment, while residues involved in interactions of individual members of the protein family with their specific target will not be conserved. The ankyrin repeats seem to belong to one predominant single family, such that consensus design is comparatively straightforward.

The repeat modules are held together by a hydrophobic interface, and thus the first (N-capping repeat or N-cap) and last repeat (C-capping repeat

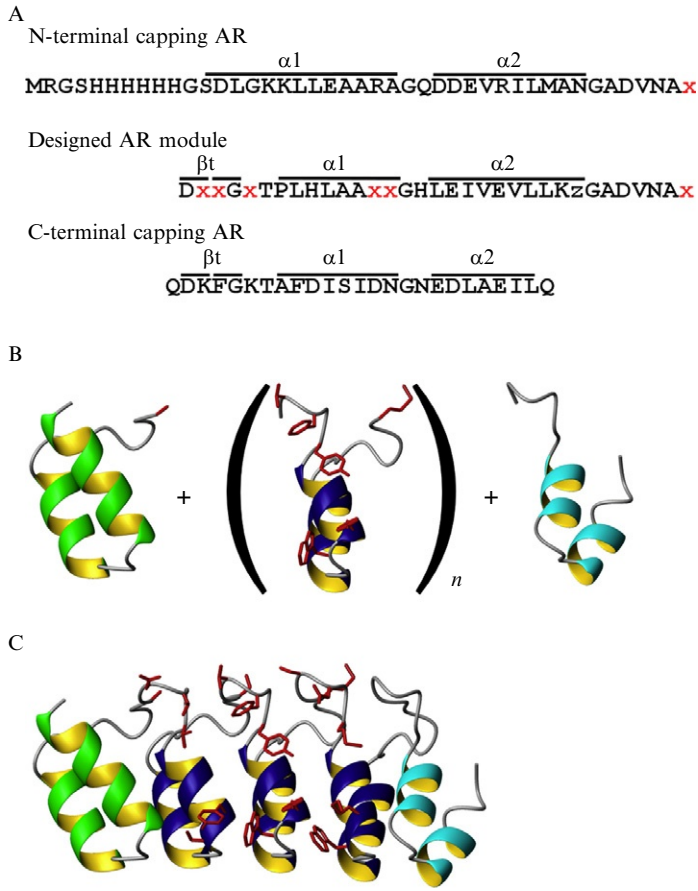

Figure 5.1 DARPin modules and typical DARPin 3D Structure. (A) Sequences of the N-terminal capping ankyrin repeat (AR), the designed AR module, and the C-terminal capping AR. The secondary structure elements are indicated above the sequences. The designed AR module consists of 26 defined framework residues, 6 randomized potential interaction residues (red x, any of the 20 natural amino acids except cysteine, glycine, or proline), and 1 randomized framework residue (z, any of the amino acids asparagine, histidine, or tyrosine). The designed AR module was derived via sequence and structure consensus analyses. (B) Schematic representation of the library generation of designed AR proteins (DARPins). Note that this assembly is represented on the protein level, whereas the real library assembly is on the DNA level. By assembling an N-terminal capping AR (green, left), varying numbers of the designed AR module (blue, middle), and a C-terminal capping AR (cyan, right), combinatorial libraries of DARPins of different repeat numbers were generated (side chains of the randomized potential interaction residues are shown in stick-mode in red). (C) Ribbon representation of the selected MBP binding DARPin off7 (colors as in B). This binder is derived from a library consisting of an N-terminal capping AR, three designed AR modules, and a C-terminal capping AR. Figure reproduced from Binz *et al.* (2004).

or C-cap) have to be special and need to present a hydrophilic outside surface exposed to the solvent. In the original design, both caps were taken from a natural protein (Binz *et al.*, 2003). More recently, this C-cap has been redesigned, based on molecular dynamics calculations, to make it more similar to the consensus, and it has been experimentally verified that the new C-cap is indeed much more resistant against thermal and denaturant-induced unfolding (Interlandi *et al.*, 2008). Crystallography (Kramer *et al.*, 2010) and NMR (Wetzel *et al.*, 2010) show that this is due to better packing of the C-cap against the internal repeats.

The "full-consensus" DARPins, where all the residues are chosen from consensus considerations, show remarkable properties. They express very well in *Escherichia coli* as soluble monomers, their stability increases with length, and those with more than three internal repeats are resistant to denaturation by boiling or guanidine hydrochloride. Full denaturation requires high temperature in 5 *M* guanidine hydrochloride (Wetzel *et al.*, 2008). Hydrogen/deuterium exchange experiments of DARPins with two and three internal repeats indicate that this high stability of the full-consensus ankyrin repeat proteins is due to the strong coupling between repeats. Some amide protons require more than a year to exchange at 37 °C (Wetzel *et al.*, 2010), highlighting the extraordinary stability of the proteins. The location of these very slowly exchanging protons indicates a very stable core structure in the DARPins that combines hydrophobic shielding with favorable electrostatic interactions.

We can consider these full-consensus DARPins as the hypothetical diversification point of a library (even though, historically, the library had been constructed first; Binz *et al.*, 2003). Thus, when diverging from a point of extremely high stability, many changes in the protein, necessary for function but potentially detrimental to stability, can be tolerated, and the outcome is still a very good protein. It appears that the experimental results confirm this hypothesis (see e.g., Binz *et al.*, 2003, 2006; Kohl *et al.*, 2003; Wetzel *et al.*, 2008).

A second reason, besides stability, for basing the DARPin library on a consensus ankyrin, as opposed to a particular naturally occurring ankyrin, was to make the library modules self-compatible (Binz *et al.*, 2003) (Fig. 5.1A and B) such that they can be assembled in any order. Such a designed repeat library module comprises fixed and variable positions. The fixed positions mainly reflect conserved framework positions, while the six variable positions mainly reflect nonconserved surface-exposed residues that can be potentially engaged in interactions with the target, as they are located on the target-binding (concave) face. The theoretical diversities of the DARPin libraries are 5.2×10^{15} or 3.8×10^{23} for two- or tree-module binders, respectively, and the actual sizes of the libraries are equal to the

number of different molecules present. We can estimate them as 10^{12} in ribosome display (Plückthun, 2011) and 10^{10} in phage display (Steiner *et al.*, 2008).

1.4. Selection technologies for DARPin libraries

DARPins have been selected from the synthetic libraries by ribosome display and phage display. Ribosome display is a potent *in vitro* method to select and evolve proteins or peptides from a naïve library with very high diversity to bind to any chosen target of interest (Hanes and Plückthun, 1997; Hanes *et al.*, 1998, 2000a; Mattheakis *et al.*, 1994). A key feature of ribosome display, in contradistinction to most other selection technologies, is that it incorporates PCR into the procedure and thus allows a convenient incorporation of a diversification ("randomization") step. Thereby, ribosome display allows refinement and affinity maturation not only of preexisting binders (Dreier *et al.*, 2011; Hanes *et al.*, 2000b; Luginbühl *et al.*, 2006; Zahnd *et al.*, 2007b) but also of the whole pool during selection from a complex library, if desired. It appears that, as the DARPins fold very well, also in cell free translation, binders are enriched somewhat faster than binders from a comparable scFv ribosome display library (Dreier and Plückthun, 2010; Hanes *et al.*, 2000a).

Using ribosome display, DARPins have been evolved to bind various targets with affinities all the way down to the picomolar range (Amstutz *et al.*, 2005; Binz *et al.*, 2004; Dreier *et al.*, 2011; Huber *et al.*, 2007; Schweizer *et al.*, 2007; Veesler *et al.*, 2009; Zahnd *et al.*, 2006, 2007b). The theoretical considerations for designing efficient off-rate selection experiments were recently summarized (Zahnd *et al.*, 2010a).

DARPins have also been selected by phage display. In filamentous phage display using fusions to the minor coat protein g3p, the protein of interest is first produced as a membrane-bound intermediate, with the domains of interest secreted to the *E. coli* periplasm but remaining still attached to the inner membrane. The g3p fusion is then taken up by the extruding phage. As DARPins fold very fast in the cytoplasm (Wetzel *et al.*, 2008), they fold before they can be transported across the membrane via the posttranslational Sec system, the normal way of secreting *E. coli* proteins. Thus, very low display rates would be observed using Sec-dependent signal sequences. However, *E. coli* has another secretion system, the signal recognition particle (SRP) dependent one, which is essentially cotranslational (Bibi, 2011; Fekkes and Driessen, 1999). Using phagemids with SRP-dependent signal sequences, phage display selection of DARPins leads to enrichment just as fast as phage display of slow folding proteins, for example, scFv fragments, using Sec-dependent phage display (Steiner *et al.*, 2006). Binders with subnanomolar K_D could be obtained from the phage display

library without affinity maturation for a variety of targets (Steiner *et al.*, 2008). For completeness, we also mention that previous attempts to achieve functional display of g3p fusions via the Tat route have proven unsuccessful (Dröge *et al.*, 2006; Nangola *et al.*, 2010; Paschke and Höhne, 2005), as the full-length p3 protein may itself be incompatible with the Tat system. However, a truncated version of p3 can support Tat-mediated phage display (Speck *et al.*, 2011).

1.5. DARPins as pure proteins

Most DARPins express well in *E. coli* in soluble form constituting up to 30% of total cellular protein (up to 200 mg per 1l of shake flask culture), and in the fermenter, multigram quantities per liter culture can be achieved (www.molecularpartners.com). Purification is thus straightforward, and for laboratory use, IMAC purification is the standard method used (Binz *et al.*, 2004). Usually, in the initial research, only few milligrams are needed, and thus the extreme overloading of an IMAC column of small capacity leads to very pure protein in a single step, as most *E. coli* contaminants are thereby competed out.

Additional purification steps are of course required when the protein is derivatized (e.g., with PEG, or fluorescent dyes) (see Section 3). For animal experiments, still higher purity is needed and absence of endotoxins needs to be secured, requiring additional washing steps and chromatography for endotoxin removal (Section 3.13).

Not only the full-consensus DARPin molecules but also most library members showed high thermodynamic stability during unfolding induced by heat or denaturants (Binz *et al.*, 2004; Kohl *et al.*, 2003) and can be brought to very high protein concentrations.

2. Applications of DARPins

2.1. DARPins in diagnostics

DARPins have been tested for their suitability in quantitative immunohistochemistry (Theurillat *et al.*, 2010), which requires high specificity in complex tissue. A DARPin specific for epidermal growth factor receptor 2 (HER2) with picomolar affinity was compared to an FDA-approved rabbit monoclonal antibody in paraffin-embedded tissue sections in tissue microarrays. HER2 gene amplification status is an important criterion to determine the optimal therapy in breast cancer. As an external reference, the HER2 amplification status was determined by fluorescence *in situ* hybridization. It was found that the DARPin detects a positive HER2

amplification status with similar sensitivity and significantly higher specificity than the FDA-approved antibody (Theurillat *et al.*, 2010). Thus, DARPins have the desired specificity characteristics for diagnostic pathology.

2.2. DARPins in tumor targeting

High affinity and specificity for a tumor cell marker is necessary but not sufficient for successful tumor targeting. Another very important issue is the quantitative enrichment at the tumor site. This, in turn, depends on the molecular format. Using DARPins, the influence of affinity and size on the efficiency of targeting was systematically investigated. DARPins are very small (molecular weight, MW 15–18 kDa) yet can easily be PEGylated (see Sections 3.3 and 3.8). For a DARPin conjugated to a PEG molecule with a nominal MW of 20 kDa, the hydrodynamic properties correspond to a MW of about 250–350 kDa (Chapman, 2002; Kubetzko *et al.*, 2005), and thus the effect of tumor targeting over a large size range could be studied. Furthermore, different point mutants binding to the same epitope of HER2 were available from the directed evolution by ribosome display, spanning affinities from 280 n*M* to 90 p*M*.

These studies showed (Zahnd *et al.*, 2010b) that there are *two* parameter regions for efficient tumor accumulation. Perhaps at first somewhat unexpected, unmodified small DARPins were found to accumulate rather well, directly proportional to affinity, with 8% ID/g after 24 h for a 90-p*M* binder in an SK-OV-3 subcutaneous mouse xenograft model. No evidence for a barrier effect was observed. The small DARPins were cleared from the blood extremely rapidly such that very high tumor to blood ratios (60:1) were measured. For bivalent DARPins (measured avidity on cells: 10 p*M*, see Section 3.12 for the methodology), a *lower* accumulation in the tumor was seen than for the monovalent counterpart (which already had a $K_D \approx 90$ p*M*), suggesting that smaller size is more important than very high avidity. Similarly, fusing a nonbinding DARPin to the anti-HER2 DARPin (K_D remains about 90 p*M*) gave the same *lowered* uptake compared to the single-domain DARPin. This lower uptake value is consistent with similar numbers obtained for antibody scFv fragments in the same tumor model (Adams *et al.*, 1993; Willuda *et al.*, 2001), and scFv fragments have the same MW as the DARPin–DARPin fusions. Thus, a very small MW seems to be a virtue, provided affinity is picomolar, thereby defining the first parameter set for efficient tumor accumulation.

The second parameter region of high tumor accumulation was found with PEGylated DARPins. The PEGylated DARPins accumulated more slowly and even better (13% ID/g after 24 h), and as might be expected from their larger size, their blood clearance was much slower, leading to smaller tumor to blood ratios. Interestingly, the importance of affinity was

diminished, with the DARPin of K_D=90 p*M* not showing a great advantage over the one with K_D=1 n*M*.

How can we rationalize these data? First, it should be emphasized that they are in excellent agreement with elegant modeling studies of Wittrup and colleagues (Schmidt and Wittrup, 2009; Thurber *et al.*, 2008), which have independently lead to very similar conclusions. If a very pronounced dependence of extravasation on MW is assumed, and that its MW cutoff is lower than that of renal filtration, then a molecule of intermediate MW would be filtered through the kidney, but would still not extravasate well. However, a molecule of small MW needs to bind to its receptor on the tumor very tightly, or it will be washed out rapidly. This affinity requirement is not as strong for very large, PEGylated molecules, which reside in the serum for much longer times. In contrast, medium sized molecules (such as scFv fragments) are still being cleared rapidly through the kidney, without reaching the tumor fast enough, because of their slower extravasation.

A series of elegant studies on quantifying tumor accumulation of mono- and multivalent scFv fragments have been reported, which have been summarized to suggest that very high affinity is disadvantageous for tumor targeting (Adams *et al.*, 2001). It should be noted, however, that in these investigations, iodine was used as a label which is removed by dehalogenases upon internalization. Thus, a higher affinity or avidity leading to more internalization will lead to *less* remaining label in the tumor (Rudnick *et al.*, 2011). In contrast, Zahnd *et al.* (2010b) used a residualizing Tc label, which will not be removed and will thus be counted, no matter whether the protein has become internalized or whether it remains on the surface. It is thus important to point out that the affinity optimum may be different for proteins that deliver a cargo to the cell (affinity should be as high as possible) versus those that should remain on the surface (there is an affinity optimum).

2.3. Approaches to targeted tumor therapy

DARPins have been used as targeting proteins in preclinical tumor models. Two examples, both using the epithelial cell adhesion molecule (EpCAM) as the target, shall be mentioned to illustrate the potential of DARPins. EpCAM is a homophilic cell adhesion molecule of 39–42 kDa, consisting of an extracellular domain with an epidermal growth factor- and a human thyroglobulin-like domain, and a short cytoplasmic domain (Trzpis *et al.*, 2007; van der Gun *et al.*, 2010). Its processing by regulated intramembrane proteolysis releases a cytoplasmic tail that activates the Wnt signaling pathway and induces transcription of c-myc and cyclins. EpCAM is an attractive tumor-associated target, as it is expressed at low levels on basolateral cell surfaces of some normal epithelia, while high levels of homogeneously distributed EpCAM are detectable on cells of epithelial tumors. Recently,

EpCAM was also identified as a marker of cancer-initiating cells (Trzpis *et al.*, 2007; van der Gun *et al.*, 2010). The favorable properties of EpCAM for cancer therapy are currently exploited in phase II clinical trials with a scFv-exotoxin A (ETA) immunotoxin (Biggers and Scheinfeld, 2008; Di Paolo *et al.*, 2003; Hussain *et al.*, 2006, 2007), which we developed previously (Di Paolo *et al.*, 2003).

There has been a lot of interest in attempting to employ small-interfering RNA (siRNA) for tumor control, but specific delivery to tumors and efficient cellular uptake of nucleic acids remain major challenges for gene-targeted cancer therapies. An anti-EpCAM DARPin was used as a carrier for siRNA complementary to the bcl-2 mRNA, a pro-apoptotic factor (Winkler *et al.*, 2009). To achieve complexation, the DARPin was genetically fused to protamine, and about 4–5 molecules siRNA could be bound per protamine.

Bivalent binders with a C-terminal leucine zipper (leading to a tail-to-tail fusion) lead to an avidity gain, while head-to-tail fusions (fused via a gly-ser linker) did not, suggesting that the former may have better matched the geometry of EpCAM on the cell (Winkler *et al.*, 2009). For all tested constructs (but best for the leucine-zipper constructs), a decrease in bcl-2 expression was observed at the mRNA and the protein level; this resulted in a significant sensitization of EpCAM-positive MCF-7 cells toward doxorubicin. Indeed, this sensitization was not observed in EpCAM-negative cells, indicating that siRNA uptake is receptor dependent (Winkler *et al.*, 2009).

Another EpCAM-specific DARPin was produced as a fusion toxin with *Pseudomonas aeruginosa* ETA and expressed in the cytoplasm of *E. coli* (Martin-Killias *et al.*, 2011; Stefan *et al.*, 2011) (cf. Section 3.13). While the DARPins have no cysteines, the disulfides in the toxin part formed spontaneously, and the protein was monomeric, yielding up to 90 mg after purification from 1 l of culture from a simple *E. coli* shake flask. The DARPin–ETA fusion was highly cytotoxic against various EpCAM-positive tumor cell lines with IC_{50} values less than 0.005 p*M*. This effect was competed by free DARPin, but not by unspecific DARPins. Upon systemic administration in athymic mice, the DARPin–ETA fusion efficiently localized to EpCAM-positive tumors to achieve maximum accumulation 48–72 h after injection, whereas an irrelevant control fusion toxin did not accumulate. Tumor targeting with the DARPin–ETA resulted in a strong antitumor response in mice bearing two different EpCAM-positive tumor xenografts, including complete regressions in some animals (Martin-Killias *et al.*, 2011). Thus, DARPin–ETA fusions deserve attention for clinical development.

While these examples have illustrated the possibility of using DARPins for the delivery of a payload to a tumor, the facile engineering of DARPins might also be exploited to create a multivalent DARPin with biological activity by itself, using either cross-linking on the same cell or between cells.

2.4. DARPins for viral retargeting

The facile engineering of DARPins, undoubtedly due to their robust folding in various fusion formats, has also been used in viral retargeting. Adenoviruses (Ads) are a family of nonenveloped viruses which contain a double-stranded DNA genome, and they have been developed as prototypes of gene vectors for gene therapy (Amalfitano and Parks, 2002), genetic immunizations (Sullivan *et al.*, 2003), and molecular-genetic imaging (Yeh *et al.*, 2011). Many studies have been reported to alter the native tropism of the virus to make Ad-mediated transgene delivery to desired cell targets both more efficient and target specific. Most studies focused on modifications of one of the major components of the Ad capsid, the fiber protein (Nicklin *et al.*, 2005). Ideally, this change in virus tropism should be achieved with technology that can realistically be scaled up and be applicable to any cell surface receptor. For this purpose, a strategy was developed with a bispecific adapter which can be produced in *E. coli* (Dreier *et al.*, 2011). In its most efficient form, it consists of four DARPins in tandem, three of which bind and wrap around the trimeric knob domain at the distal end of the protruding Ad fibers (while also blocking binding to the natural receptor CAR), while the fourth DARPin binds to the cellular target of interest. This strategy was tested with a HER2-binding DARPin. The adaptors showed a significant increase in cell-specific transduction, measured by luciferase activity (Dreier *et al.*, 2011). This new strategy of altering the natural tropism of Ad5 with rationally designed adapters holds great promise for future developments in gene therapy.

While the Ad genome remains episomal, lentiviral vectors lead to stable integration and transgene expression in nondividing cells. Again, the challenge is to achieve cell-specific retargeting by recognition of a specific surface antigen. Cell entry is dependent on two viral glycoproteins, hemagglutinin (H) and fusion protein (F), for example, in measles virus (MV) (Yanagi *et al.*, 2006). By using lentiviral vectors expressing MV-H and MV-F, and specifically creating a variety of fusions MV-H to HER2-specific DARPins, infection of HER2 expressing cells could be obtained (Münch *et al.*, 2011). All H-DARPin fusion proteins were efficiently expressed on the cell surface and incorporated into lentiviral vectors at a more uniform rate than scFvs, perhaps because of the more robust folding within the fusion protein. The vectors only transduced HER2-positive cells, while HER2-negative cells remained untransduced. Highest titers were observed with one particular anti-HER2 DARPin binding to the membrane distal domain of HER2. When these DARPin-carrying viral vectors were applied *in vivo* systemically in a mouse tumor xenograft model, exclusive gene expression was observed in HER2 positive tumor tissue, while control vectors mainly transduced cells in spleen and liver (Münch *et al.*, 2011). Thus, DARPins are a promising route to engineer the specificity of lentiviral vectors for therapy.

2.5. DARPins in other approaches

We will only mention briefly other approaches of potential therapeutic significance. For example, DARPins have been selected to bind to IgE or its receptor FcεRIα (Baumann *et al.*, 2010; Eggel *et al.*, 2009, 2011). DARPins have also been selected against several kinases (Amstutz *et al.*, 2005, 2006; Bandeiras *et al.*, 2008), and this may provide the basis for novel sensor systems to be able to follow internal signaling events, to monitor the success of therapeutic agents. It can be expected that the broad formatting options of DARPins will be advantageous for future developments.

2.6. DARPins in the clinic

DARPins with very high affinity have been selected against vascular endothelial growth factor VEGF (www.molecularpartners.com) and were developed for intraocular formulation. They have entered two clinical phase I/II trials in two ocular indications, wet age-related macular degeneration (wet AMD) (clinicaltrials.gov/ct2/show/NCT01086761) and diabetic macular edema (clinicaltrials.gov/ct2/show/NCT01042678).

At the time of writing, first data from the wet AMD trial are released (Wolf *et al.*, 2011), a phase I/II, open-label, noncontrolled, multicentre trial. The clinical study with DARPin MP0112 assessed the safety and preliminary efficacy measured by visual acuity, fluorescein angiography, and color fundus photography during 16 weeks. MP0112 is an extremely potent VEGF inhibitor and, because of its superior biophysical properties, can be concentrated to extremely high molar concentrations, and shows a long ocular half-life. It is suggested from these studies that dosing frequency in patients may be reduced three to fourfold, compared to current standard therapy with ranibizumab (Lucentis), an anti-VEGF Fab fragment. DARPin MP0112 was found safe and well tolerated. DARPin MP0112 represents a very promising new anti-VEGF treatment option with potential in various retinal diseases. It is a direct demonstration how the biophysical properties of the protein translate to benefit for the patient.

3. Protocols for DARPins in Biomedical Applications

The selection of DARPins from libraries using ribosome display (Dreier and Plückthun, 2011; Zahnd *et al.*, 2007a) or phage display (Steiner *et al.*, 2008) as well as their straightforward biochemical characterization (Binz *et al.*, 2003, 2004) have been described elsewhere. Thus, we will concentrate on methods for coupling DARPins with fluorescent labels and PEG, using both conventional coupling reactions and the introduction

of nonnatural amino acids for the use of "click chemistry." We then describe the use of the labeled proteins for quantitating their binding on cells using kinetic methods. Finally, we describe the expression of DARPin–toxin fusion proteins.

3.1. Stoichiometric cysteine labeling with maleimide-coupled fluorescent probes

By design, DARPins do not have any cysteine residues. Using site-directed mutagenesis, a cysteine is typically inserted in front or just behind the unstructured N-terminal $RGSH_6$ tag, or at the C-terminus of the DARPin, without affecting the stability or affinity (Fig. 5.1C).

For quantitative labeling with a maleimide-containing fluorophore, any disulfides that may have spontaneously formed need to be first reduced to free thiols. The reduction and the subsequent coupling reactions are therefore performed in a nitrogen atmosphere in a glove box to avoid reoxidation of the free thiols, which is a prerequisite to approximate quantitative yields. The following protocol describes the batch reaction for preparing 1 mg stoichiometrically labeled DARPin. DARPins, which are expressed and purified by Ni-NTA as described before (Binz *et al.*, 2004), are diluted in 500 µl of degassed Tris-buffered saline (TBS; 25 m*M* Tris(hydroxymethyl)-aminomethane (Tris), 150 m*M* sodium chloride, pH 7.5) to a concentration of 100 µ*M*. A 50 m*M* stock solution of Tris(2-carboxyethyl)phosphine (TCEP-HCl, Thermo Fisher Scientific) is freshly prepared in water (it will have a pH of ca. pH 2.5) and needs to be neutralized by the addition of potassium hydroxide. While thiol-containing reductants (such as dithiothreitol or β-mercaptoethanol) need to be separated before coupling, low concentrations of TCEP hardly interfere with the coupling reaction of small fluorophores (Getz *et al.*, 1999), and a twofold molar excess of fresh TCEP over protein is sufficient to completely reduce all cysteine residues in 30 min at room temperature at the concentrations specified.

Alexa Fluor-488-C5-maleimide (Invitrogen) is dissolved in dimethylformamide (DMF) (10 mg/ml) by sonication and can be stored over months at −80 °C. About 7 µl of this solution is subsequently added in a twofold molar excess to the protein solution (100 µ*M*, 500 µl), and the coupling is performed for 1 h at room temperature.

All subsequent purification steps are carried out under normal atmosphere while the labeled protein is constantly protected from light. The reaction mix is desalted on a NAP-5 bench top column (GE Healthcare) in phosphate-buffered saline (PBS) pH 7.1 to remove more than 98% of the unreacted Alexa Fluor-488 dye.

Alexa Fluor-488 and other small dyes, which introduce an additional negative charge to the labeled conjugate, are suitable for achieving separation of the conjugate from the unlabeled DARPin by ion exchange

chromatography (IEX). For separation of labeling products, a Mono-Q 5/50 GL column (GE Healthcare), equilibrated with Buffer A (50 m*M* Tris–HCl, pH 8.3, 10 m*M* NaCl), is used and all labeling species are loaded until the initial salt peak has been eluted. For a DARPin of unknown elution behavior, a linear elution gradient of Buffer B (50 m*M* Tris–HCl, pH 8.3, 1 *M* NaCl) is applied over 1 h. Once the elution behavior of the labeled DARPin is known, the gradient can be replaced by an optimized step gradient. The elution is monitored by the absorbance at 280 nm for the DARPin and 495 nm for the Alexa Fluor-488 dye, and fractions of 500 µl are collected on an ÄKTA Explorer FPLC instrument (GE Healthcare). The unlabeled DARPin, with a high 280 nm and no detectable 495 nm absorbance, elutes first and is followed by the labeled DARPin, which shows high absorbance at both wavelengths.

Peak fractions of the labeled species are pooled and, after desalting, the labeling efficiency is measured in a spectrophotometer by determining the molar ratio of Alexa Fluor-488 to DARPin within the conjugate, [$Alexa_{488}$]/[DARPin], where

$$[\mathrm{Alexa}_{488}] = \frac{A_{495}}{\varepsilon_{\mathrm{Alexa@495}}} \quad \text{and} \quad [\mathrm{DARPin}] = \frac{A_{280} - (A_{495} \times 0.11)}{\varepsilon_{\mathrm{DARPin}}}$$

Here, $\varepsilon_{\mathrm{Alexa@495}}$ is the molar absorbance (=71,000) of the dye at 495 nm (where the protein absorption is negligible) and $\varepsilon_{\mathrm{DARPin}}$ is the molar absorbance of at the DARPin at 280 nm. The term $A_{495} \times 0.11$ is the absorbance of the dye at 280 nm, which is calculated from its absorbance measured at 495 nm.

For DARPins with few aromatic residues, the Alexa Fluor-488 dye may contribute much of the absorbance at 280 nm, and consequently, the labeling efficiency is difficult to determine. Thus, an alternative method is to resolve the labeled fraction by electrophoresis on a 20% sodium dodecyl sulfate polyacrylamide gel (SDS-PAGE). DARPins labeled with Alexa Fluor-488 will shift toward higher mass and can be identified with a fluorescence camera, while the ratio of labeled to unlabeled form of the protein can be estimated by staining with Coomassie Brilliant Blue.

3.2. Stoichiometric N-terminal labeling with succinimidyl-ester coupled fluorescent probes

To circumvent the need for cysteine mutagenesis, DARPins can also be selectively labeled at the N-terminal amino group. Because of the favorable orientation of the N-cap of a DARPin (Fig. 5.1C), an N-terminally coupled fluorophore is unlikely to interfere with the binding properties of the DARPin. The acylation of primary amines occurs essentially through the nonprotonated form and is thus dependent on the respective pK_a value.

While the N-terminal amine has a pK_a of 8, the ε-amino group of a fully exposed lysine side chain has a pK_a of 10.5 (even though buried ones can be significantly lower). There are typically several lysine residues in the protein and their combined reaction with the dye is thus significant even at lower pH. Therefore, reaction conditions (time, pH, and excess of dye) must be set to favor selectivity of the N-terminal amino group labeling and not the yield of the conjugate.

Purified DARPin is diluted to a concentration of 100 μ*M* in 500 μl PBS, pH 7.1. Alexa Fluor-488 carboxylic acid succinimidyl ester (Invitrogen), dissolved in DMF, is added in a threefold molar excess over protein and the coupling reaction is incubated for 80 min at room temperature. The coupling reaction is terminated by rebuffering in TBS on a NAP-5 column.

Monolabeled DARPins (which will be predominantly labeled at the N-terminus) can be purified, similar to cysteine-labeled DARPins, by anion exchange chromatography (Section 3.1). The elution profile is monitored at 280 and 495 nm and will show multiple peaks. The most prominent peak is likely to represent the N-terminally labeled fraction, while the other peaks correspond to different lysine-labeled species. Unlabeled, monolabeled, and multiply labeled protein can be distinguished based on the ratio of A_{280} and A_{495}.

If the assignment of the N-terminally labeled fraction is not unambiguous, a deliberate labeling at higher pH may further help to distinguish between the N-terminal and the lysine-labeled DARPin conjugates. For this purpose, all amines of the DARPin are coupled at pH 8.1 and the products are analyzed analogously by IEX. In the chromatogram overlay of both reactions, the relative amount of N-terminally labeled DARPin is diminished at pH 8.1, while all lysine-labeled DARPin fractions will increase. Exact sequence information of the DARPin modifications can be obtained by analyzing the fractions by means of peptide fragmentation on tandem MS/MS mass spectrometry.

3.3. Quantitative PEGylation of DARPins

Large polymeric moieties such as coupled PEG may interfere with binding of DARPins to their epitopes, but only if their attachment point is very close to the paratope. Thus, the coupling of PEG must be site-specific and the attachment point must be remote. In this case, no effect on the off-rate should be found, and only a small effect on the on-rate, for reasons established elsewhere (Kubetzko *et al.*, 2005).

The covalent coupling of maleimide-functionalized PEG to cysteine residues is the most convenient method for site-specific PEGylation. In contrast to small fluorophores, the reactivity of functionalized PEG decreases with higher concentrations and higher MW of the polymer due to the increasing viscosity of the reaction mix.

Here, we provide a protocol for reacting DARPins in solution with a 40-kDa, 2-branched maleimide-PEG, (SUNBRIGHT GL2-400MA, NOF Corporation). The DARPin is purified according to Binz *et al.* (2004) and diluted to a concentration of 200 μ*M* in 2.5 ml degassed PBS, pH 7.1.

The maleimide coupling is performed under oxygen-free conditions in a glove box with a nitrogen or argon atmosphere, analogously to the cysteine labeling with fluorophores (Section 3.1). For the PEGylation of DARPins, DTT instead of TCEP is used as reducing agent, due to the straightforward removal of DTT by desalting on a bench top column, which may be inefficient for TCEP (Shafer *et al.*, 2000). While low concentrations of TCEP do not significantly hinder the coupling of small dyes (Section 3.1), TCEP measurably affects the rate of the PEGylation reaction, and at long reaction times, side reactions can occur.

A 1 *M* stock solution of DTT is prepared freshly in degassed H_2O right before use, and 12.5 μl of DTT stock solution is added to the protein solution (200 μ*M*, 2.5 ml), vortexed, and incubated for 1 h at room temperature. Meanwhile, a PD-10 gravity-flow column (GE Healthcare) is equilibrated with degassed and N_2-flushed PBS, pH 7.1. DTT is removed from the protein by elution with 3.5 ml PBS pH 7.1. A twofold molar excess of a freshly prepared solution of maleimide-PEG is added directly into the reaction mix, and coupling is performed for 4 h at room temperature.

All following steps are carried out again in normal atmosphere. Free PEG and uncoupled DARPins can be efficiently removed from PEGylated DARPins by anion exchange chromatography. An ÄKTA Explorer FPLC system equipped with a Mono-Q 5/50 GL column is suitable to purify a total of up to 20 mg PEGylated DARPin per run. The reaction mix is diluted threefold to reduce ionic strength and loaded on the Mono-Q column equilibrated in Buffer A (50 m*M* Tris–HCl, pH 8.3, 10 m*M* NaCl), and the reaction mix is loaded. After unbound PEG has eluted in the flow through, a linear salt gradient of Buffer B (50 m*M* Tris–HCl, pH 8.3, 1 *M* NaCl) is applied over 1 h to efficiently separate the reaction products. The absorbance profile is monitored at 280 nm for DARPin, and fractions of 500 μl are collected. Due to charge shielding or the steric interference of PEG with the DARPin-column interaction, the PEGylated DARPins will elute before the non-PEGylated DARPins from the Mono-Q column. For identification of the different reaction products, the collected fractions are resolved on a 12% SDS-PAGE and stained with Coomassie Brilliant Blue and, optionally, with barium iodide solution for visualization of PEG (Kurfürst, 1992). The PEG-coupled DARPin run at a higher MW than the calculated one of the conjugate. On gel filtration, they even show a hydrodynamic radius corresponding to an apparent MW of about 300,000 Da (Chapman, 2002; Kubetzko *et al.*, 2005).

As the Tris buffer used in the IEX purification is toxic, it needs to be exchanged prior to *in vivo* applications. Therefore, PEGylated DARPins are rebuffered in PBS pH 7.4 by size exclusion chromatography on an FPLC system equipped with a Superdex200 10/300 GL column (GE Healthcare).

3.4. Introduction to "Click chemistry"

The azide-alkyne Huisgen cycloaddition ("Click chemistry") offers an orthogonal coupling reaction that does not interfere with functionalities present in proteins (Fig. 5.2). The formation of triazole can be catalyzed by Cu(I) (Deiters *et al.*, 2004; Wang *et al.*, 2003) or by the use of a strained alkyne (Debets *et al.*, 2010). This strategy especially allows the additional use of a cysteine residue to directionally couple two different ligands site-specifically (e.g., PEG, and a radioligand or fluorophore). This approach does require, however, the introduction of either an alkyne or an azido functionality into the protein by the use of nonnatural amino acids. The group of D. Tirrell has shown that the methionine analogs azidohomoalanine

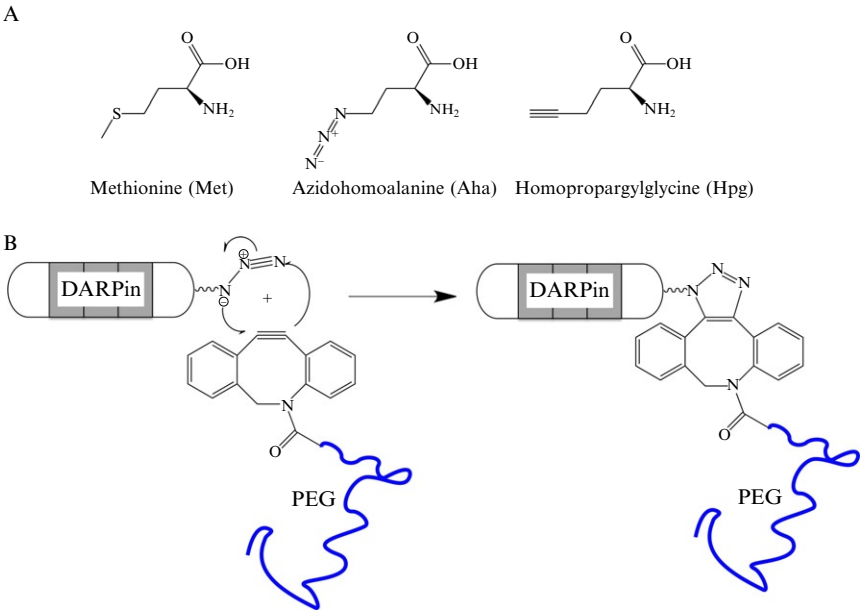

Figure 5.2 (A) Amino acid analogs which can be incorporated as a methionine analog in *E. coli*. (B) Azide-alkyne Huisgen cycloaddition ("click chemistry") of an azidohomoalanine residue, incorporated instead of the initiator methionine (the sole Met in the protein), with aza-dibenzocyclooctyne (DBCO), which is available coupled to polyethylene glycol (PEG).

(Aha) or homopropargylglycine (Hpg) can be incorporated in recombinant proteins in *E. coli* in high yields by the use of a Met auxotroph strain (Kiick *et al.*, 2002; Teeuwen *et al.*, 2009).

DARPins are ideal proteins for the N-terminal modification with methionine analogs *in vivo* as only few (mostly only one) internal methionines are present in the protein backbone. The single methionine present in the N-cap is not required and can be routinely exchanged (Simon *et al.*, 2012). The initiator Met, which is not cleaved in front of the subsequent Arg (of the $RGSH_6$ tag), is thus the only position where a clickable methionine analog will be incorporated. If a unique Met is desired at another position, the choice of a small second amino acid (Ala, Gly, Ser) leads to efficient cleavage of the initiator Met (Wang *et al.*, 2008).

3.5. Expression of "clickable" DARPins

DARPins can be conveniently labeled with the unnatural amino acids Aha or Hpg using a metabolic incorporation strategy. In a first step, the methionine in the conserved N-cap of the DARPins at position 34 can be exchanged for leucine using universal Quikchange™ (Stratagene, La Jolla, USA) primers without altering the biochemical properties of the DARPin molecule. The resulting M34L DARPin mutant is subcloned into a vector containing the *lacI* gene under the stronger $lacI^q$ promoter control and transformed into the methionine auxotroph *E. coli* B-strain B834 DE3 (F^- *ompT hsdS*$_B$ ($r_B^- m_B^-$) *gal dcm met* (DE3)) (Novagen) for expression. An overnight culture is used to inoculate 2×YT medium supplemented with 1% glucose and 100 µg/ml ampicillin at an OD_{600} of 0.1. Cells are cultivated for 2–3 h at 37 °C with agitation. Once an optical density of 1.0–1.2 is reached, the expression cultures are centrifuged (5000×*g*, 10 min, 4 °C) and the cells washed thoroughly for three times using ice-cold 0.9% NaCl solution by resuspension with a pipette in order to deplete all extracellular methionine. The cells are constantly cooled on ice to stop further cell growth during the wash procedure. Finally, the cells are reinoculated in M9 minimal medium (SelenoMethionine Medium Base plus Nutrient Mix [a nutrient mix with 19 amino acids], Molecular Dimensions Ltd., UK), containing 100 µg/ml ampicillin, and are supplemented further with Hpg (Chiralix, Nijmegen, Netherlands) or Aha (Bapeks, Riga, Latvia) (40 mg/l) from a sterile filtered stock solution. The expression cultures are incubated for 15 min at 30 °C in a shaker in order to additionally deplete all intracellular methionine pools of *E. coli*. The cells are subsequently induced using 1 m*M* isopropyl-β-D-thio-galactopyranoside (IPTG) and incubated for 4 h at 30 °C for expression of "clickable" DARPins. Finally, all cells are pelleted by centrifugation, resuspended in PBS, and pelleted again. The resulting pellets are snap-frozen and stored at −80 °C.

3.6. IMAC purification of "clickable" DARPins

The pellets are thawed on ice with HBS_W buffer (50 m*M* Hepes, 150 m*M* NaCl, 20 m*M* imidazole, pH 8.0) supplemented with 2 mg/l lysozyme and lysed for 3–4 times using a French® pressure cell press (Aminco) at 1200 psi. The lysate is centrifuged (28,000 × *g*, 4 °C, 1 h) and the supernatants are applied on pre-packed bench top Ni-NTA immobilized metal ion affinity chromatography (IMAC) columns (Qiagen). The proteins are washed with 20 column volumes (CV) of HBS_LS (50 m*M* Hepes, 20 m*M* NaCl, 20 m*M* imidazole, pH 8.0) followed by HBS_HS (50 m*M* Hepes, 1 *M* NaCl, 20 m*M* imidazole, pH 8.0) washes for 20 CV. Next, the IMAC columns are again washed with HBS_W (see above, 10 CVs) and the proteins are eluted using PBS_E (PBS, 300 m*M* imidazole, pH 7.4). The fractions are quantified using a Nanodrop spectrophotometer (Thermo Scientific). The proteins are thoroughly dialyzed against PBS overnight, aliquoted, snap-frozen, and stored for "click"-labeling. Usual protein yields are 25–30 mg DARPin per liter expression culture depending on the clone and expression time after induction.

3.7. Analysis of "clickable" DARPins

Incorporation of the nonnatural amino acids Aha or Hpg can be analyzed using N-terminal protein sequencing (Edman degradation). Briefly, 5–15 µl of the protein sample is diluted in 100 µl 0.1% TFA and loaded on a Prosorb Sample Preparation Cartridge (ABI), washed two times with 0.1% TFA, and transferred onto a PVDF membrane. The N-terminal amino acid composition is then analyzed using a PROCISE cLC 492 device. The nonnatural amino acids appear as new peaks that cannot be assigned to methionine: Whereas methionine gives a maximum signal at a retention time of 17.5 min, the maximum of either Hpg or Aha is approximately 16 min. Only very low amounts of methionine, in the noise range, can be detected after successful incorporation of the nonnatural amino acids.

The "clickable" DARPins can in addition be quantified via amino acid hydrolysis using the AccQ Tag Ultra kit (Waters). Ten microliters of the protein sample is dried followed by a vapor phase hydrolysis in 6 *M* HCl for 24 h at 110 °C under argon. The dry sample is taken up in 50 µl borate buffer and 10 µl are derivatized according to the manufacturer's recommendations, and the amino acids are separated on a UPLC system (Waters). Additionally, norvaline is taken as an internal standard and transferrin as a control protein. The analysis normally reveals no methionine present in the "clickable" DARPins after hydrolysis as a result of the substitution by the methionine surrogates.

3.8. Site-specific PEGylation of DARPins using Cu-free "click chemistry"

PEGylation of DARPins at the N-terminus is performed by using azadibenzocyclooctyne (DBCO)-PEG-20kDa (Click Chemistry Tools) for Cu-free labeling (Debets *et al.*, 2010). "Clickable" azido-DARPins (containing an N-terminal Aha) (100μ*M* in PBS) are mixed with two- to threefold molar excess of DBCO-PEG-20kDa from a 5m*M* DBCO-PEG-20kDa stock in PBS. At these concentrations, after 3–4h at room temperature or overnight at 4°C (without the necessity of agitation), the yield reaches about 70–80% (Fig. 5.3). Increasing the temperature leads to increased reaction rates. The maximal yield after extended reaction times (48h at room temperature) is usually about 85%, where the residual non-PEGylated 15% can be assigned to DARPin molecules whose N-terminal methionine substitute Aha has been posttranslationally cleaved off by the *E. coli* methionine aminopeptidase *in vivo* (Wang *et al.*, 2008), as detected by N-terminal sequencing.

The reaction is not depending on particular buffers, can be performed in a broad pH range, and can even be used in combination with buffers containing imidazole from the elution of IMAC purification straight away. The PEGylated product is detected as a band shift of the DARPins using 15% SDS-PAGE as described above for the cys-maleimide PEGylation.

3.9. Purification of "click" PEGylated DARPins

Anion exchange is used to separate PEGylated from non-PEGylated DARPins and free DBCO-PEG (Seely and Richey, 2001), as described for the cys-maleimide PEGylation (Section 3.3). In order to reduce viscosity and ionic strength, the proteins are diluted in Buffer A (50m*M* Hepes, 20m*M*

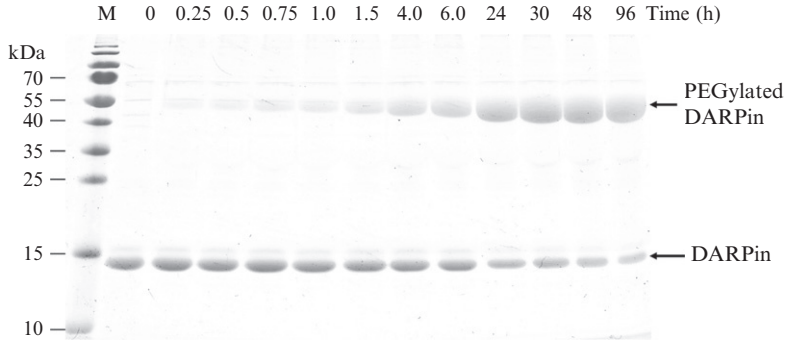

Figure 5.3 Time course of the Cu(I)-independent "click reaction": reaction of a DARPin containing an N-terminal Aha with DBCO-PEG-20kDa (15% SDS-PAGE, stained with Coomassie Brilliant Blue).

NaCl, pH 8.5) and loaded on a MonoQ 5/10 column (GE Healthcare) connected to a pre-equilibrated ÄKTA Explorer FPLC system (GE Healthcare). The proteins are eluted using a linear gradient of Buffer B (50 m*M* Hepes, 1 *M* NaCl, pH 8.5). Whereas the non-PEGylated DARPins remain bound to the anion exchange column, the PEGylated DARPins are eluted early as a result of the covalent attachment of PEG and can be quantitatively eluted at lower salt concentrations as described elsewhere (Seely and Richey, 2001). Using this method, unreacted DBCO-PEG-20 kDa is eluted in the flow through and can thus be separated from the proteins. The fractions containing the PEGylated DARPins are pooled and desalted or dialyzed against PBS for further use.

3.10. Measurement of DARPin binding affinity to whole cells

Frequently, DARPins binding to surface receptors have been obtained by selection to the purified receptor, and thus it is important to determine the affinity to the receptor in the natural context on intact viable cells. Binding might be influenced by the local membrane environment, the accessibility of particular epitopes, and posttranslational modifications of the receptors.

Unfortunately, there are technical challenges with many methods when applying them to viable cells. The most common method, the measurement of equilibrium binding of radioactively labeled ligand by radioimmunoassay, has a large experimental error because of the high number of washing steps and the difficulty in discriminating between intact cells and damaged cells with permeable membranes. We therefore elaborated methodology based on fluorescence-activated cell sorting (FACS). By gating on forward and side scatter, we can selectively measure binding to live cells.

To obtain correct values for ligand binding parameters from surface receptors such as HER2, internalization has to be minimized. We thus routinely preincubate the cells with 0.1% sodium azide (blocking ATP-driven endocytosis) for 30 min at 37 °C before incubating with DARPins and have this concentration of sodium azide present during all steps. It was found that by this means, >95% inhibition of HER2 internalization is achieved while keeping reasonable viability of BT474 cells. Under these conditions, DARPins completely dissociate over time, with almost no fluorescence remaining associated with the cells after extended time. However, it has to be noted that the efficient inhibition of internalization could be highly cell-type- and receptor dependent. For other cell lines or receptor–ligand systems, different classes of inhibitors of endocytosis, for example, monodansyl cadaverine, phenylarsine oxide, chlorpromazine, amantadine, monensin, or K^+-depletion, may be the preferred choice (Vercauteren *et al.*, 2010). It is therefore recommended to define the most suitable conditions for suppression of endocytosis in every particular experimental setup.

3.11. Determination of the dissociation constant by equilibrium titration on cells

Equilibrium titration experiments can in principle be used to quantify the number of receptors on the cell surface as well as for determination of ligand affinity. It should be noted, however, that this method is limited to K_D values in the nanomolar range and cannot be used for tighter-binding ligands (see Section 3.12).

Since reaching equilibrium is a prerequisite for the accurate determination of dissociation constants, it is important that incubation with the labeled ligand proceeds for a sufficient period of time, which may range from a few minutes to several hours, depending on ligand affinity, temperature, and analyte concentration. In a typical equilibrium titration experiment, cells (e.g., BT474 or SKOV3 overexpressing the HER2 receptor) are incubated at concentration of 1×10^6 cells/ml with the labeled ligand, for example, DARPin-Alexa Fluor-488 conjugates, at concentration varying from 50 p*M* to 100 n*M* at room temperature for 1 h or longer, if required (Fig. 5.4). The incubation is maintained under conditions with minimized

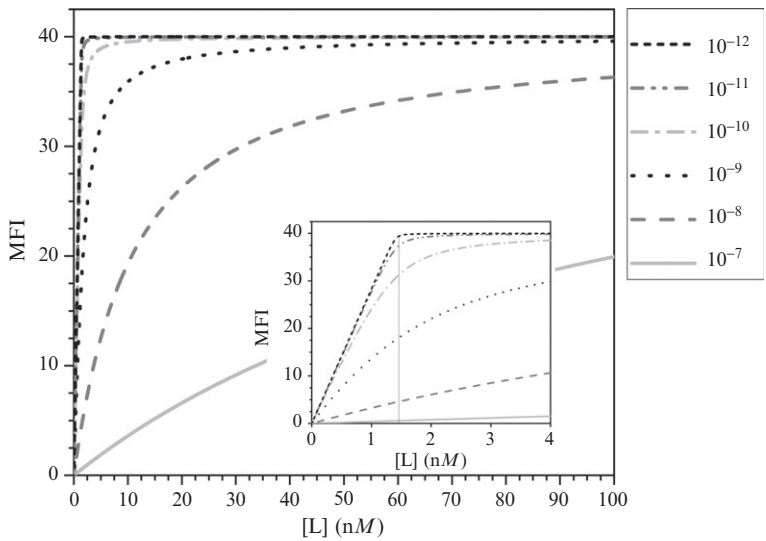

Figure 5.4 Equilibrium titration of cellular receptors with labeled ligands. Simulated data of mean fluorescent intensity are shown according to Eq. (5.2), as they are typically obtained when measuring binding of a fluorescently labeled DARPin by FACS. It can be seen that a reliable determination of K_D by curve fitting is only possible for affinities weaker than 1 n*M*, otherwise the curves become practically identical (independent of K_D), especially when considering scatter in the data. Conversely, with high-affinity data, the equivalence point allows precise determination of the receptor concentration (insert, vertical line indicating the equivalence point). When the number of cells is known, the receptor number per cell is directly obtained.

receptor internalization in PBS containing 1% (w/v) BSA and 0.1% (w/v) sodium azide (abbreviated PBSBA). For each concentration point, a 1-ml cell-DARPin suspension is subjected to FACS analysis on the FL1 detector (530/20 band pass filter) of an appropriate instrument equipped with a 488-nm argon laser. Before measurements, the cells are briefly washed once with ice-cold PBS to suppress the background arising from the unspecific binding of labeled ligand. If necessary, control samples are preincubated with 100-fold excess of unlabeled DARPins, and the recorded values are subsequently subtracted from total binding to correct for unspecific background.

The data are usually analyzed by nonlinear regression to a simplified binding isotherm:

$$\mathrm{MFI} = \mathrm{MFI}_{\max} \frac{[\mathrm{L}]}{[\mathrm{L}] + K_{\mathrm{D}}} \tag{5.1}$$

where MFI is the measured mean fluorescence intensity (corrected for the background), $\mathrm{MFI}_{\max}$ the background-corrected plateau value corresponding to saturated receptors, [L] the concentration of the labeled ligand, and K_{D} the dissociation constant to be determined. Equation (5.1) does not take ligand depletion into account, which occurs with tightly binding ligands at stoichiometric ratios with receptor. A more accurate version is the following equation

$$\mathrm{MFI} = \frac{\mathrm{MFI}_{\max}}{[\mathrm{C}]_{\max}} \left(\frac{[\mathrm{R}] + [\mathrm{L}] + K_{\mathrm{D}}}{2} - \sqrt{\left(\frac{[\mathrm{R}] + [\mathrm{L}] + K_{\mathrm{D}}}{2} \right)^2 - [\mathrm{L}] \cdot [\mathrm{R}]} \right) \tag{5.2}$$

where the variables are as in Eq. (5.1), and [R] is the molar concentration of receptor. The value $\mathrm{MFI}_{\max}/[\mathrm{C}]_{\max}$ is a proportionality constant determined from the fit, relating the maximal response to the maximal concentration of receptor–ligand complex C.

It has to be noted that determinations of dissociation constants by equilibrium titration possesses some inherent limitations. For instance, if the analyte concentration is far above its K_{D}, only inaccurate affinity determinations are possible, as the receptor–ligand complexes are saturated upon titration (Fig. 5.4). For high-affinity binders (K_{D} below 100 p*M*), this problem cannot be simply solved by dilution, as the sensitivity limits of most detection methods will be reached. However, if the ligand affinity is too low (K_{D} above 100 n*M*), the rate of dissociation is usually too high for ligand to remain bound to the receptor during washing steps and analysis. Although this problem can be mitigated by an indirect measurement setup employing the unlabeled ligand of interest in combination with a labeled high-affinity competitor, such a high-affinity binder is often not available. Hence,

accurate measurements for equilibrium dissociation constant determination can be obtained with ligand concentrations in the range of the K_D, and experimental constraints demand that this has to be around 1–100 n*M*.

However, equilibrium titration with labeled ligand can be readily used to estimate (from the equivalence point in the titration) the total number of receptors expressed on cells (Zahnd *et al.*, 2010b). This is possible because the receptor concentration equals the concentration of the titrating ligand at the equivalence point of a binding isotherm recorded under conditions where the molar concentration of both the receptor and the ligand are sufficiently above the K_D. The situation with $K_D \ll [R]$ and $K_D > [R]$ is shown with simulated data in Fig. 5.4.

3.12. Determination of kinetic parameters of binding on cells

Measuring affinities of picomolar ligands by equilibrium titration is very inaccurate, inasmuch as for sensitivity reasons it would require ligand concentrations in the range far above the K_D value. Thus, it is preferable to determine the dissociation constant indirectly as the ratio of the dissociation rate constant and the association rate constant. Also, the knowledge of these kinetic parameters often contains additional valuable information.

The rate of association, defined as

$$\frac{d[C]}{dt} = k_{on} \cdot [L] \cdot [R] \tag{5.3}$$

where [L] is the DARPin ligand, [R] is the uncomplexed receptor, [C] is the receptor–ligand complex, and k_{on} (in units of $M^{-1}s^{-1}$) is the association rate constant, can be determined by following the binding of labeled DARPin to cells during defined time intervals. The determination of k_{on} does require an estimate of the receptor number per cell and knowledge of the cell number, which is best achieved by titration at high concentrations (Fig. 5.4, inset). Note that [C] is proportional to MFI (more precisely, the receptor-specific part of the signal)

The rate of dissociation is defined as

$$-\frac{d[C]}{dt} = k_{off} \cdot [C] \tag{5.4}$$

where k_{off} is the dissociation rate constant (units of s^{-1}). At equilibrium, the sum of both rates is zero, and thus

$$K_D = \frac{[L] \cdot [R]}{[C]} = \frac{k_{off}}{k_{on}} \tag{5.5}$$

For on-rate determinations, BT474 cells are incubated at a concentration of 1×10^6 cells/ml with 2.5, 7.5, and 22.5 nM DARPin-Alexa Fluor-488 conjugates in PBSBA at room temperature for defined time intervals, ranging from 1 to 60 min. For each time point, a 1-ml aliquot of cells is withdrawn and subjected to FACS. Since the applied concentrations of the labeled ligand conjugates are very low, and since the time resolution of the measurement is to be maintained to ensure the accuracy of the on-rate determination, the samples are processed without further washing. For each time point, at least 10^4 intact cells (gated as a uniform population on a FSC/SSC scatter plot) are counted, and the MFI is recorded. Parameters are fitted with a monoexponential equation

$$\mathrm{MFI} = \mathrm{MFI}_{\max}\left(1 - \mathrm{e}^{-k_{\mathrm{obs}}t}\right) \tag{5.6}$$

where k_{obs} is the observed association rate constant, and

$$k_{\mathrm{obs}} = k_{\mathrm{on}}\cdot[\mathrm{L}] + k_{\mathrm{off}} \tag{5.7}$$

In an association-type experiment where k_{off} is not immeasurably small, the increment of MFI combines the ligand binding with the concomitant ligand dissociation and thus, more precisely, describes the rate of reaching equilibrium in a given receptor–ligand system. As a consequence, the actual k_{on} can only be determined in conjunction with the preceding measurement of the dissociation rate constant k_{off}. Typically, the ligands display on-rate constants in the range of 10^5 to $10^6\,M^{-1}\mathrm{s}^{-1}$. An example of an on-rate determination experiment is shown in Fig. 5.5A.

To perform off-rate determinations, the receptors are saturated with the labeled ligand, which is subsequently allowed to dissociate, and the amount of remaining cell-bound ligand is repeatedly monitored by FACS at defined time points, usually spanning the interval from 1 min to several hours, depending on dissociation rate. To prevent rebinding of dissociated ligand to the free receptor, which would prevent a correct determination of k_{off}, a large excess (100-fold) of unlabeled ligand should be included in the reaction, which will block each unoccupied receptor after dissociation of the labeled ligand. For instance, BT474 cells at a concentration of 1×10^6 cells/100 µl are saturated with 50 nM anti-HER2 DARPin-Alexa Fluor-488 conjugates for 60 min on ice in PBSBA. Thereafter, the cells are washed extensively (at least three times) with ice-cold PBSBA to remove unbound labeled DARPin. The cells are then diluted 10-fold to a final concentration of 1×10^6 cells/ml in PBSBA and gently agitated at room temperature for the duration of the measurement. To prevent reassociation of dissociated DARPin-Alexa Fluor-488 conjugate, an excess of competitor (100 nM unlabeled DARPin) must be added. Under these conditions, complete loss of fluorescence over time should be seen, indicating that

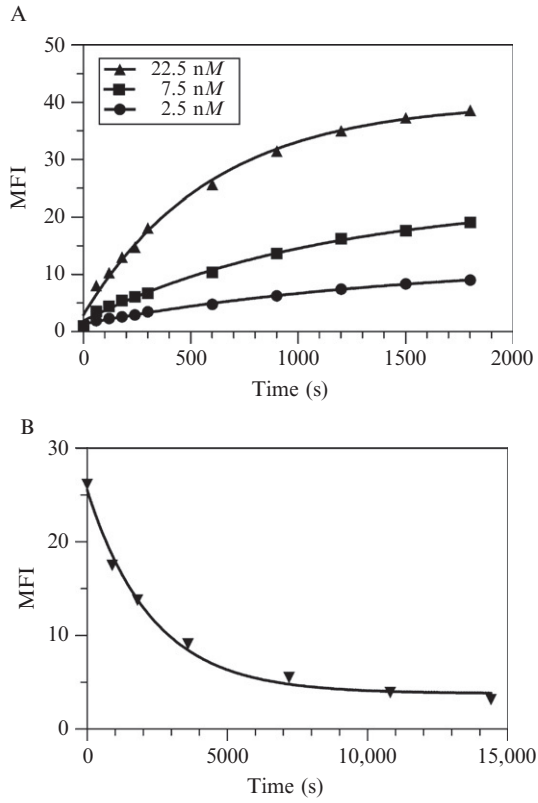

Figure 5.5 Association and dissociation kinetics of DARPin-Alexa Fluor-488 conjugate, binding to HER2 on BT474 cells. The mean fluorescence intensity (MFI), as recorded by FACS, is monitored as a function of time. (A) The DARPin-HER2 association is monitored at three DARPin-Alexa Fluor-488 concentrations as indicated. The association rate constant is evaluated with Eqs. (5.6) and (5.7). (B) DARPin dissociation of BT474 cells preloaded with DARPin-Alexa Fluor-488 after dilution in fresh buffer in the presence of unlabeled competitor DARPin. The dissociation rate constant is evaluated with Eq. (5.8). The K_D is determined with Eq. (5.5).

both rebinding and receptor internalization have been successfully prevented. Before FACS measurements, the cells are briefly washed once with ice-cold PBS. A typical dissociation experiment is shown in Fig. 5.5B.

Collected data are fitted with the following equation

$$\mathrm{MFI} = (\mathrm{MFI}_{\max} - \mathrm{MFI}_{\infty})\mathrm{e}^{-k_{\mathrm{off}}t} \tag{5.8}$$

where $\mathrm{MFI}_{\max}$ is the initial value, and MFI_{∞} is the plateau value after long dissociation.

In principle, the experiment can be carried out also in the reverse fashion, by preincubating the cells (1×10^6 cells/100 µl) with 50 n*M* unlabeled DARPin. Upon washing cells three times to remove unbound DARPins, the dissociation is started by competing with 100 n*M* of Alexa Fluor-488-conjugated DARPin. In this case, the dissociation of the unlabeled DARPin is measured by the increase of fluorescence, as dissociation is much slower than the very rapid association of the labeled DARPin under these conditions. Irrespective of experimental setup, the dissociation rates for potent receptor-binding DARPins are typically in the range of 10^{-3}–10^{-5} s^{-1}.

3.13. Expression and purification of DARPin–toxin fusion proteins

Potential applications for DARPins include the targeted delivery of protein toxins (Martin-Killias *et al.*, 2011). *P. aeruginosa* ETA (Siegall *et al.*, 1989) has been widely used for this purpose. The DARPin replaces the natural N-terminal domain of the toxin, which mediates binding to the α_2 macroglobulin receptor. DARPins are fused via a 12-amino acid linker $(GSG_4)_2$ to the 40-kDa truncated form of $ETA_{252–608}$KDEL (ETA″), which was cloned as described (Di Paolo *et al.*, 2003; Wels *et al.*, 1992). ETA″ comprises residues Glu252–Pro608 (numbering of the mature protein), fused to a C-terminal His_6 tag followed by KDEL (denoted $ETA_{252–608}$KDEL or ETA″). For purification and detection, the construct in addition contains an MRGS-His_6 tag at the N-terminus.

The DARPin–toxin fusion proteins are expressed in soluble form in the cytoplasm of *E. coli*, using a vector derived from pQE30 (Qiagen), but containing the *lac* repressor gene under the control of the stronger $lacI^q$ promoter. The DARPin–ETA″ fusion proteins are expressed in soluble form in the *E. coli* strain BL21 (DE3) (Stratagene). Precultures are grown in 2×YT broth (16 g/l tryptone, 10 g/l yeast extract, 5 g/l NaCl) containing 100 µg/ml ampicillin and 1% glucose, with shaking overnight at 37 °C. Cultures are diluted in Terrific Broth (Tartoff and Hobbs, 1987) (12 g/l tryptone, 24 g/l yeast extract, 4 ml/l glycerol, 17 m*M* KH_2PO_4, and 72 m*M* K_2HPO_4) containing 50 µg/ml ampicillin and 0.1% glucose to OD_{600} 0.1 and grown at 37 °C. Upon reaching OD_{600} of 1.2, the temperature is reduced to 30 °C and recombinant protein production is induced with 1 m*M* IPTG. Cells are harvested 5 h after induction, washed once with TBS_{400} (50 m*M* Tris–HCl, 400 m*M* NaCl, pH 8.0, at 4 °C), snap-frozen in liquid N_2, and stored at −80 °C or used directly for downstream processing.

For purification, the bacteria are resuspended in TBS_{400}_W (50 m*M* Tris–HCl, pH 7.4, 400 m*M* NaCl, 20 m*M* imidazole) and lysed with a TS 1.1-kW cell disruptor (Constant Systems Ltd.) using a pressure of 35 MPa. The cell lysate is centrifuged (48,000×*g*, 30 min at 4 °C) and filtered

(pore size 0.22 μm) prior to purifying the fusion toxins from the supernatant by a gravity-flow Ni-NTA superflow column (Qiagen). After loading, the column is washed with 10 CV of low-salt TBS_W (50 m*M* Tris–HCl, pH 7.4, 50 m*M* NaCl, 20 m*M* imidazole) and high-salt TBS_W (50 m*M* Tris–HCl, pH 7.4, 1 *M* NaCl, 20 m*M* imidazole) to remove unspecifically bound material, followed by 10 CV of PBS pH 7.4 containing 20 m*M* imidazole. DARPin–ETA″ is eluted with PBS containing 250 m*M* imidazole and dialyzed twice against PBS at 4 °C. The protein yield after dialysis is up to 90 mg/l of bacterial culture.

For *in vivo* applications, the DARPin–ETA″ fusion toxins are further purified to eliminate endotoxin. To this end, an additional washing step is performed during IMAC purification using 150 column volumes PBS containing 20 m*M* imidazole and 0.1% Triton-X-114, a nonionic detergent which efficiently solubilizes endotoxin at a temperature below its cloud point of 23 °C (Reichelt *et al.*, 2006; Zimmerman *et al.*, 2006). Next, the monomeric fraction of DARPin–ETA″ is separated by size exclusion chromatography using a Superdex-200 10/300 GL column (GE Healthcare) and further depleted of residual endotoxin by passages over an EndoTrap Red affinity column (Hyglos). The final endotoxin content is determined using the Limulus amebocyte lysate endochrome kit (Charles River).

The DARPin contains no cysteine by design, but the ETA″ possesses two disulfide bonds. As the fusion protein is expressed in the reducing cytoplasm of *E. coli*, it is important to verify that proper disulfides have indeed formed. It is noteworthy that their formation normally proceeds spontaneously with excellent yield (Martin-Killias *et al.*, 2011) (cf. Section 2.3), presumably by air oxidation.

SS-bond formation can be quantified according to Hansen *et al.* (2007). Like in the classic Ellman test (Ellman, 1959), the free thiols of L-cysteine are detected by incubation for 30 min at room temperature with 0.36 m*M* 4,4′-dithiodipyridine (4-DPS), a reagent which stoichiometrically reacts with free thiols forming two 4-thiopyridone (4-TP) molecules. The reaction is stopped by the addition of HCl to a final concentration of 0.2 *M*. However, unlike in the classic Ellman test, here 4-TP is assayed by analyzing 20-μl aliquots by reverse phase HPLC on a 250 mm NUCLEOSIL® 120–5 C_{18} column (Macherey-Nagel), using isocratic elution at a flow rate of 1 ml/min in 50 m*M* potassium acetate, pH 4.0. Peaks are detected at 324 nm.

First, a series of standards from 1 to 133 μ*M* cysteine is prepared in 100 m*M* citrate, 0.2 m*M* ethylenediaminetetraacetic acid, and 6 *M* urea at pH 4.5. The standard curve can be calculated from the peak integral of the 4-TP peaks.

The protein of interest is treated with 4-DPS in the presence of 8 *M* urea to detect the free thiols in the protein. In parallel, the same procedure is applied to a sample which had been reduced with sodium borohydride (BH), a strong reducing reagent, to expose all apparent thiols (Hansen *et al.*, 2007). To avoid pressure buildup in the reduced sample tubes, caused by

hydrogen development, lids are pierced with a needle. Excess BH is rapidly and quantitatively removed using 1.8*M* HCl, and the lower pH at the same time preserves the integrity of the thiol groups. It is important to keep the incubation time in presence 4-DPS identical for the reduced and nonreduced samples by adding 4-DPS to both samples at the same time to assure accuracy. Analysis of DARPin–ETA″ typically revealed less than 10% free thiols, suggesting over 90% correctly formed disulfide bridges.

ACKNOWLEDGMENT

Work in the author's laboratory on establishing the methods was supported by the Swiss National Science Foundation and Swiss Anti-Cancer League (Krebsliga Schweiz; KFS 02448-08-2009).

REFERENCES

Adams, G. P., McCartney, J. E., Tai, M. S., Oppermann, H., Huston, J. S., Stafford, W. F., 3rd, Bookman, M. A., Fand, I., Houston, L. L., and Weiner, L. M. (1993). Highly specific in vivo tumor targeting by monovalent and divalent forms of 741F8 anti-c-erbB-2 single-chain Fv. *Cancer Res.* **53,** 4026–4034.

Adams, G. P., Schier, R., McCall, A. M., Simmons, H. H., Horak, E. M., Alpaugh, R. K., Marks, J. D., and Weiner, L. M. (2001). High affinity restricts the localization and tumor penetration of single-chain Fv antibody molecules. *Cancer Res.* **61,** 4750–4755.

Amalfitano, A., and Parks, R. J. (2002). Separating fact from fiction: Assessing the potential of modified adenovirus vectors for use in human gene therapy. *Curr. Gene Ther.* **2,** 111–133.

Amstutz, P., Binz, H. K., Parizek, P., Stumpp, M. T., Kohl, A., Grütter, M. G., Forrer, P., and Plückthun, A. (2005). Intracellular kinase inhibitors selected from combinatorial libraries of designed ankyrin repeat proteins. *J. Biol. Chem.* **280,** 24715–24722.

Amstutz, P., Koch, H., Binz, H. K., Deuber, S. A., and Plückthun, A. (2006). Rapid selection of specific MAP kinase-binders from designed ankyrin repeat protein libraries. *Protein Eng. Des. Sel.* **19,** 219–229.

Bandeiras, T. M., Hillig, R. C., Matias, P. M., Eberspaecher, U., Fanghänel, J., Thomaz, M., Miranda, S., Crusius, K., Pütter, V., Amstutz, P., Gulotti-Georgieva, M., Binz, H. K., *et al.* (2008). Structure of wild-type Plk-1 kinase domain in complex with a selective DARPin. *Acta Crystallogr. D Biol. Crystallogr.* **64,** 339–353.

Baumann, M. J., Eggel, A., Amstutz, P., Stadler, B. M., and Vogel, M. (2010). DARPins against a functional IgE epitope. *Immunol. Lett.* **133,** 78–84.

Bibi, E. (2011). Early targeting events during membrane protein biogenesis in Escherichia coli. *Biochim. Biophys. Acta* **1808,** 841–850.

Biggers, K., and Scheinfeld, N. (2008). VB4-845, a conjugated recombinant antibody and immunotoxin for head and neck cancer and bladder cancer. *Curr. Opin. Mol. Ther.* **10,** 176–186.

Binz, H. K., Stumpp, M. T., Forrer, P., Amstutz, P., and Plückthun, A. (2003). Designing repeat proteins: Well-expressed, soluble and stable proteins from combinatorial libraries of consensus ankyrin repeat proteins. *J. Mol. Biol.* **332,** 489–503.

Binz, H. K., Amstutz, P., Kohl, A., Stumpp, M. T., Briand, C., Forrer, P., Grütter, M. G., and Plückthun, A. (2004). High-affinity binders selected from designed ankyrin repeat protein libraries. *Nat. Biotechnol.* **22,** 575–582.

Binz, H. K., Kohl, A., Plückthun, A., and Grütter, M. G. (2006). Crystal structure of a consensus-designed ankyrin repeat protein: Implications for stability. *Proteins* **65,** 280–284.

Bork, P. (1993). Hundreds of ankyrin-like repeats in functionally diverse proteins: Mobile modules that cross phyla horizontally? *Proteins* **17,** 363–374.

Chapman, A. P. (2002). PEGylated antibodies and antibody fragments for improved therapy: A review. *Adv. Drug Deliv. Rev.* **54,** 531–545.

Debets, M. F., van Berkel, S. S., Schoffelen, S., Rutjes, F. P., van Hest, J. C., and van Delft, F. L. (2010). Aza-dibenzocyclooctynes for fast and efficient enzyme PEGylation via copper-free (3+2) cycloaddition. *Chem. Commun. (Camb.)* **46,** 97–99.

Deiters, A., Cropp, T. A., Summerer, D., Mukherji, M., and Schultz, P. G. (2004). Site-specific PEGylation of proteins containing unnatural amino acids. *Bioorg. Med. Chem. Lett.* **14,** 5743–5745.

Di Paolo, C., Willuda, J., Kubetzko, S., Lauffer, I., Tschudi, D., Waibel, R., Plückthun, A., Stahel, R. A., and Zangemeister-Wittke, U. (2003). A recombinant immunotoxin derived from a humanized epithelial cell adhesion molecule-specific single-chain antibody fragment has potent and selective antitumor activity. *Clin. Cancer Res.* **9,** 2837–2848.

Dreier, B., and Plückthun, A. (2010). Ribosome display, a technology for selecting and evolving proteins from large libraries. *Methods Mol. Biol.* **687,** 283–306.

Dreier, B., and Plückthun, A. (2011). Ribosome display: A technology for selecting and evolving proteins from large libraries. *Methods Mol. Biol.* **687,** 283–306.

Dreier, B., Mikheeva, G., Belousova, N., Parizek, P., Boczek, E., Jelesarov, I., Forrer, P., Plückthun, A., and Krasnykh, V. (2011). Her2-specific multivalent adapters confer designed tropism to adenovirus for gene targeting. *J. Mol. Biol.* **405,** 410–426.

Dröge, M. J., Boersma, Y. L., Braun, P. G., Buining, R. J., Julsing, M. K., Selles, K. G., van Dijl, J. M., and Quax, W. J. (2006). Phage display of an intracellular carboxylesterase of Bacillus subtilis: Comparison of Sec and Tat pathway export capabilities. *Appl. Environ. Microbiol.* **72,** 4589–4595.

Eggel, A., Baumann, M. J., Amstutz, P., Stadler, B. M., and Vogel, M. (2009). DARPins as bispecific receptor antagonists analyzed for immunoglobulin E receptor blockage. *J. Mol. Biol.* **393,** 598–607.

Eggel, A., Buschor, P., Baumann, M. J., Amstutz, P., Stadler, B. M., and Vogel, M. (2011). Inhibition of ongoing allergic reactions using a novel anti-IgE DARPin-Fc fusion protein. *Allergy* **66,** 961–968.

Ellman, G. L. (1959). Tissue sulfhydryl groups. *Arch. Biochem. Biophys.* **82,** 70–77.

Fekkes, P., and Driessen, A. J. (1999). Protein targeting to the bacterial cytoplasmic membrane. *Microbiol. Mol. Biol. Rev.* **63,** 161–173.

Forrer, P., Stumpp, M. T., Binz, H. K., and Plückthun, A. (2003). A novel strategy to design binding molecules harnessing the modular nature of repeat proteins. *FEBS Lett.* **539,** 2–6.

Forrer, P., Binz, H. K., Stumpp, M. T., and Plückthun, A. (2004). Consensus design of repeat proteins. *ChemBioChem* **5,** 183–189.

Getz, E. B., Xiao, M., Chakrabarty, T., Cooke, R., and Selvin, P. R. (1999). A comparison between the sulfhydryl reductants tris(2-carboxyethyl)phosphine and dithiothreitol for use in protein biochemistry. *Anal. Biochem.* **273,** 73–80.

Glockshuber, R., Malia, M., Pfitzinger, I., and Plückthun, A. (1990). A comparison of strategies to stabilize immunoglobulin Fv-fragments. *Biochemistry* **29,** 1362–1367.

Hanes, J., and Plückthun, A. (1997). *In vitro* selection and evolution of functional proteins by using ribosome display. *Proc. Natl. Acad. Sci. USA* **94,** 4937–4942.

Hanes, J., Jermutus, L., Weber-Bornhauser, S., Bosshard, H. R., and Plückthun, A. (1998). Ribosome display efficiently selects and evolves high-affinity antibodies *in vitro* from immune libraries. *Proc. Natl. Acad. Sci. USA* **95,** 14130–14135.

Hanes, J., Jermutus, L., and Plückthun, A. (2000a). Selecting and evolving functional proteins *in vitro* by ribosome display. *Methods Enzymol.* **328,** 404–430.

Hanes, J., Schaffitzel, C., Knappik, A., and Plückthun, A. (2000b). Picomolar affinity antibodies from a fully synthetic naive library selected and evolved by ribosome display. *Nat. Biotechnol.* **18,** 1287–1292.

Hansen, R. E., Ostergaard, H., Norgaard, P., and Winther, J. R. (2007). Quantification of protein thiols and dithiols in the picomolar range using sodium borohydride and 4,4′-dithiodipyridine. *Anal. Biochem.* **363,** 77–82.

Huber, T., Steiner, D., Röthlisberger, D., and Plückthun, A. (2007). In vitro selection and characterization of DARPins and Fab fragments for the co-crystallization of membrane proteins: The Na(+)-citrate symporter CitS as an example. *J. Struct. Biol.* **159,** 206–221.

Hussain, S., Plückthun, A., Allen, T. M., and Zangemeister-Wittke, U. (2006). Chemosensitization of carcinoma cells using epithelial cell adhesion molecule-targeted liposomal antisense against bcl-2/bcl-xL. *Mol. Cancer Ther.* **5,** 3170–3180.

Hussain, S., Plückthun, A., Allen, T. M., and Zangemeister-Wittke, U. (2007). Antitumor activity of an epithelial cell adhesion molecule targeted nanovesicular drug delivery system. *Mol. Cancer Ther.* **6,** 3019–3027.

Interlandi, G., Wetzel, S. K., Settanni, G., Plückthun, A., and Caflisch, A. (2008). Characterization and further stabilization of designed ankyrin repeat proteins by combining molecular dynamics simulations and experiments. *J. Mol. Biol.* **375,** 837–854.

Kiick, K. L., Saxon, E., Tirrell, D. A., and Bertozzi, C. R. (2002). Incorporation of azides into recombinant proteins for chemoselective modification by the Staudinger ligation. *Proc. Natl. Acad. Sci. USA* **99,** 19–24.

Knappik, A., Ge, L., Honegger, A., Pack, P., Fischer, M., Wellnhofer, G., Hoess, A., Wölle, J., Plückthun, A., and Virnekäs, B. (2000). Fully synthetic human combinatorial antibody libraries (HuCAL) based on modular consensus frameworks and CDRs randomized with trinucleotides. *J. Mol. Biol.* **296,** 57–86.

Kobe, B., and Kajava, A. V. (2000). When protein folding is simplified to protein coiling: The continuum of solenoid protein structures. *Trends Biochem. Sci.* **25,** 509–515.

Kohl, A., Binz, H. K., Forrer, P., Stumpp, M. T., Plückthun, A., and Grütter, M. G. (2003). Designed to be stable: Crystal structure of a consensus ankyrin repeat protein. *Proc. Natl. Acad. Sci. USA* **100,** 1700–1705.

Kramer, M. A., Wetzel, S. K., Plückthun, A., Mittl, P. R., and Grütter, M. G. (2010). Structural determinants for improved stability of designed ankyrin repeat proteins with a redesigned C-capping module. *J. Mol. Biol.* **404,** 381–391.

Kubetzko, S., Sarkar, C. A., and Plückthun, A. (2005). Protein PEGylation decreases observed target association rates via a dual blocking mechanism. *Mol. Pharmacol.* **68,** 1439–1454.

Kurfürst, M. M. (1992). Detection and molecular weight determination of polyethylene glycol-modified hirudin by staining after sodium dodecyl sulfate-polyacrylamide gel electrophoresis. *Anal. Biochem.* **200,** 244–248.

Li, J., Mahajan, A., and Tsai, M. D. (2006). Ankyrin repeat: A unique motif mediating protein-protein interactions. *Biochemistry* **45,** 15168–15178.

Luginbühl, B., Kanyo, Z., Jones, R. M., Fletterick, R. J., Prusiner, S. B., Cohen, F. E., Williamson, R. A., Burton, D. R., and Plückthun, A. (2006). Directed evolution of an anti-prion protein scFv fragment to an affinity of 1 pM and its structural interpretation. *J. Mol. Biol.* **363,** 75–97.

Martin-Killias, P., Stefan, N., Rothschild, S., Plückthun, A., and Zangemeister-Wittke, U. (2011). A novel fusion toxin derived from an EpCAM-specific designed ankyrin repeat protein has potent antitumor activity. *Clin. Cancer Res.* **17,** 100–110.

Mattheakis, L. C., Bhatt, R. R., and Dower, W. J. (1994). An in vitro polysome display system for identifying ligands from very large peptide libraries. *Proc. Natl. Acad. Sci. USA* **91,** 9022–9026.

Münch, R. C., Mühlebach, M. D., Schaser, T., Kneissl, S., Jost, C., Plückthun, A., Cichutek, K., and Buchholz, C. J. (2011). DARPins: An efficient targeting domain for lentiviral vectors. *Mol. Ther.* **19,** 686–693.

Nangola, S., Minard, P., and Tayapiwatana, C. (2010). Appraisal of translocation pathways for displaying ankyrin repeat protein on phage particles. *Protein Expr. Purif.* **74,** 156–161.

Nicklin, S. A., Wu, E., Nemerow, G. R., and Baker, A. H. (2005). The influence of adenovirus fiber structure and function on vector development for gene therapy. *Mol. Ther.* **12,** 384–393.

Pancer, Z., Amemiya, C. T., Ehrhardt, G. R., Ceitlin, J., Gartland, G. L., and Cooper, M. D. (2004). Somatic diversification of variable lymphocyte receptors in the agnathan sea lamprey. *Nature* **430,** 174–180.

Paschke, M., and Höhne, W. (2005). A twin-arginine translocation (Tat)-mediated phage display system. *Gene* **350,** 79–88.

Plückthun, A. (2012). Ribosome display: A perspective. *Methods Mol. Biol.* **805,** 3–28.

Plückthun, A., and Moroney, S. E. (2005). Modern antibody technology: The impact on drug development. *In* "Modern Biopharmaceuticals," (J. Knäblein, ed.) Vol. 3, pp. 1147–1186. Wiley-VCH, Weinheim (4 vols).

Reichelt, P., Schwarz, C., and Donzeau, M. (2006). Single step protocol to purify recombinant proteins with low endotoxin contents. *Protein Expr. Purif.* **46,** 483–488.

Rudnick, S. I., Lou, J., Shaller, C. C., Tang, Y., Klein-Szanto, A. J., Weiner, L. M., Marks, J. D., and Adams, G. P. (2011). Influence of affinity and antigen internalization on the uptake and penetration of anti-HER2 antibodies in solid tumors. *Cancer Res.* **71,** 2250–2259.

Schmidt, M. M., and Wittrup, K. D. (2009). A modeling analysis of the effects of molecular size and binding affinity on tumor targeting. *Mol. Cancer Ther.* **8,** 2861–2871.

Schweizer, A., Roschitzki-Voser, H., Amstutz, P., Briand, C., Gulotti-Georgieva, M., Prenosil, E., Binz, H. K., Capitani, G., Baici, A., Plückthun, A., and Grütter, M. G. (2007). Inhibition of caspase-2 by a designed ankyrin repeat protein: Specificity, structure, and inhibition mechanism. *Structure* **15,** 625–636.

Sedgwick, S. G., and Smerdon, S. J. (1999). The ankyrin repeat: A diversity of interactions on a common structural framework. *Trends Biochem. Sci.* **24,** 311–316.

Seely, J. E., and Richey, C. W. (2001). Use of ion-exchange chromatography and hydrophobic interaction chromatography in the preparation and recovery of polyethylene glycol-linked proteins. *J. Chromatogr. A* **908,** 235–241.

Shafer, D. E., Inman, J. K., and Lees, A. (2000). Reaction of tris(2-carboxyethyl)phosphine (TCEP) with maleimide and alpha-haloacyl groups: Anomalous elution of TCEP by gel filtration. *Anal. Biochem.* **282,** 161–164.

Siegall, C. B., Chaudhary, V. K., FitzGerald, D. J., and Pastan, I. (1989). Functional analysis of domains II, Ib, and III of Pseudomonas exotoxin. *J. Biol. Chem.* **264,** 14256–14261.

Simon, M., Zangemeister-Wittke, U. and Plückthun, A. (2012). Facile double-functionalization of designed ankyrin repeat proteins using click and thiol chemistries. *Bioconjug. Chem.* (in press).

Skerra, A., and Plückthun, A. (1988). Assembly of a functional immunoglobulin Fv fragment in *Escherichia coli*. *Science* **240,** 1038–1041.

Speck, J., Arndt, K. M., and Müller, K. M. (2011). Efficient phage display of intracellularly folded proteins mediated by the TAT pathway. *Protein Eng. Des. Sel.* **24,** 473–484.

Stefan, N., Martin-Killias, P., Wyss-Stoeckle, S., Honegger, A., Zangemeister-Wittke, U., and Plückthun, A. (2011). DARPins recognizing the tumor-associated antigen EpCAM

selected by phage and ribosome display and engineered for multivalency. *J. Mol. Biol.* **413,** 826–843.

Steiner, D., Forrer, P., Stumpp, M. T., and Plückthun, A. (2006). Signal sequences directing cotranslational translocation expand the range of proteins amenable to phage display. *Nat. Biotechnol.* **24,** 823–831.

Steiner, D., Forrer, P., and Plückthun, A. (2008). Efficient selection of DARPins with sub-nanomolar affinities using SRP phage display. *J. Mol. Biol.* **382,** 1211–1227.

Stumpp, M. T., Forrer, P., Binz, H. K., and Plückthun, A. (2003). Designing repeat proteins: Modular leucine-rich repeat protein libraries based on the mammalian ribonuclease inhibitor family. *J. Mol. Biol.* **332,** 471–487.

Sullivan, N. J., Geisbert, T. W., Geisbert, J. B., Xu, L., Yang, Z. Y., Roederer, M., Koup, R. A., Jahrling, P. B., and Nabel, G. J. (2003). Accelerated vaccination for Ebola virus haemorrhagic fever in non-human primates. *Nature* **424,** 681–684.

Tartoff, K. D., and Hobbs, C. A. (1987). Improved media for growing plasmid and cosmid clones. *Bethesda Res. Labs Focus* **9,** 12–14.

Teeuwen, R. L., van Berkel, S. S., van Dulmen, T. H., Schoffelen, S., Meeuwissen, S. A., Zuilhof, H., de Wolf, F. A., and van Hest, J. C. (2009). "Clickable" elastins: Elastin-like polypeptides functionalized with azide or alkyne groups. *Chem. Commun. (Camb.)* 4022–4024.

Theurillat, J. P., Dreier, B., Nagy-Davidescu, G., Seifert, B., Behnke, S., Zurrer-Hardi, U., Ingold, F., Plückthun, A., and Moch, H. (2010). Designed ankyrin repeat proteins: A novel tool for testing epidermal growth factor receptor 2 expression in breast cancer. *Mod. Pathol.* **23,** 1289–1297.

Thurber, G. M., Schmidt, M. M., and Wittrup, K. D. (2008). Antibody tumor penetration: Transport opposed by systemic and antigen-mediated clearance. *Adv. Drug Deliv. Rev.* **60,** 1421–1434.

Trzpis, M., McLaughlin, P. M., de Leij, L. M., and Harmsen, M. C. (2007). Epithelial cell adhesion molecule: More than a carcinoma marker and adhesion molecule. *Am. J. Pathol.* **171,** 386–395.

van der Gun, B. T., Melchers, L. J., Ruiters, M. H., de Leij, L. F., McLaughlin, P. M., and Rots, M. G. (2010). EpCAM in carcinogenesis: The good, the bad or the ugly. *Carcinogenesis* **31,** 1913–1921.

Veesler, D., Dreier, B., Blangy, S., Lichière, J., Tremblay, D., Moineau, S., Spinelli, S., Tegoni, M., Plückthun, A., Campanacci, V., and Cambillau, C. (2009). Crystal structure of a DARPin neutralizing inhibitor of lactococcal phage TP901-1: Comparison of DARPin and camelid VHH binding mode. *J. Biol. Chem.* **384,** 30718–30726.

Vercauteren, D., Vandenbroucke, R. E., Jones, A. T., Rejman, J., Demeester, J., De Smedt, S. C., Sanders, N. N., and Braeckmans, K. (2010). The use of inhibitors to study endocytic pathways of gene carriers: Optimization and pitfalls. *Mol. Ther.* **18,** 561–569.

Walker, R. G., Willingham, A. T., and Zuker, C. S. (2000). A Drosophila mechanosensory transduction channel. *Science* **287,** 2229–2234.

Wang, Q., Chan, T. R., Hilgraf, R., Fokin, V. V., Sharpless, K. B., and Finn, M. G. (2003). Bioconjugation by copper(I)-catalyzed azide-alkyne [3+2] cycloaddition. *J. Am. Chem. Soc.* **125,** 3192–3193.

Wang, A., Winblade Nairn, N., Johnson, R. S., Tirrell, D. A., and Grabstein, K. (2008). Processing of N-terminal unnatural amino acids in recombinant human interferon-beta in Escherichia coli. *ChemBioChem* **9,** 324–330.

Wels, W., Harwerth, I. M., Mueller, M., Groner, B., and Hynes, N. E. (1992). Selective inhibition of tumor cell growth by a recombinant single-chain antibody-toxin specific for the erbB-2 receptor. *Cancer Res.* **52,** 6310–6317.

Wetzel, S. K., Settanni, G., Kenig, M., Binz, H. K., and Plückthun, A. (2008). Folding and unfolding mechanism of highly stable full-consensus ankyrin repeat proteins. *J. Mol. Biol.* **376,** 241–257.

Wetzel, S. K., Ewald, C., Settanni, G., Jurt, S., Plückthun, A., and Zerbe, O. (2010). Residue-resolved stability of full-consensus ankyrin repeat proteins probed by NMR. *J. Mol. Biol.* **402,** 241–258.

Willuda, J., Kubetzko, S., Waibel, R., Schubiger, P. A., Zangemeister-Wittke, U., and Plückthun, A. (2001). Tumor targeting of mono-, di- and tetravalent anti-p185^{HER-2} miniantibodies multimerized by self-associating peptides. *J. Biol. Chem.* **276,** 14385–14392.

Winkler, J., Martin-Killias, P., Plückthun, A., and Zangemeister-Wittke, U. (2009). EpCAM-targeted delivery of nanocomplexed siRNA to tumor cells with designed ankyrin repeat proteins. *Mol. Cancer Ther.* **9,** 2674–2683.

Wolf, S., Souied, E. H., Mauget-Faysse, M., Devin, F., Patel, M., Wolf-Schnurrbusch, U. E., and Stumpp, M. T. (2011). Phase I MP0112 wet AMD study: Results of a single escalating dose study with DARPin MP0112 in wet AMD. Abstracts of Papers, 2011 Annual Meeting of the Association for Research in Vision and Ophthalmology (ARVO 2011), Fort Lauderdale, FL, Poster 1655.

Wörn, A., and Plückthun, A. (2001). Stability engineering of antibody single-chain F_v fragments. *J. Mol. Biol.* **305,** 989–1010.

Yanagi, Y., Takeda, M., Ohno, S., and Seki, F. (2006). Measles virus receptors and tropism. *Jpn. J. Infect. Dis.* **59,** 1–5.

Yeh, H. H., Ogawa, K., Balatoni, J., Mukhapadhyay, U., Pal, A., Gonzalez-Lepera, C., Shavrin, A., Soghomonyan, S., Flores, L., 2nd, Young, D., Volgin, A. Y., Najjar, A. M., *et al.* (2011). Molecular imaging of active mutant L858R EGF receptor (EGFR) kinase-expressing nonsmall cell lung carcinomas using PET/CT. *Proc. Natl. Acad. Sci. USA* **108,** 1603–1608.

Zahnd, C., Pécorari, F., Straumann, N., Wyler, E., and Plückthun, A. (2006). Selection and characterization of Her2 binding-designed ankyrin repeat proteins. *J. Biol. Chem.* **281,** 35167–35175.

Zahnd, C., Amstutz, P., and Plückthun, A. (2007a). Ribosome display: Selecting and evolving proteins in vitro that specifically bind to a target. *Nat. Methods* **4,** 269–279.

Zahnd, C., Wyler, E., Schwenk, J. M., Steiner, D., Lawrence, M. C., McKern, N. M., Pecorari, F., Ward, C. W., Joos, T. O., and Plückthun, A. (2007b). A designed ankyrin repeat protein evolved to picomolar affinity to Her2. *J. Mol. Biol.* **369,** 1015–1028.

Zahnd, C., Sarkar, C. A., and Plückthun, A. (2010a). Computational analysis of off-rate selection experiments to optimize affinity maturation by directed evolution. *Protein Eng. Des. Sel.* **23,** 175–184.

Zahnd, C., Kawe, M., Stumpp, M. T., de Pasquale, C., Tamaskovic, R., Nagy-Davidescu, G., Dreier, B., Schibli, R., Binz, H. K., Waibel, R., and Plückthun, A. (2010b). Efficient tumor targeting with high-affinity designed ankyrin repeat proteins: Effects of affinity and molecular size. *Cancer Res.* **70,** 1595–1605.

Zimmerman, T., Petit Frère, C., Satzger, M., Raba, M., Weisbach, M., Döhn, K., Popp, A., and Donzeau, M. (2006). Simultaneous metal chelate affinity purification and endotoxin clearance of recombinant antibody fragments. *J. Immunol. Methods* **314,** 67–73.